J. Appl. Comput. Mech., 7(1) (2021) 277-291
DOI: 10.22055/JACM.2020.31836.1924

ISSN: 2383-4536
jacm.scu.ac.ir

Shahid Chamran University of Ahvaz

Journal of Applied and Computational Mechanics

Research Paper

Thermoelastic Model with Higher-order Time-derivatives and Two Phase-lags for an Infinitely Long Cylinder under Initial Stress and Heat Source

Anouar Saidi[1,2], Ahmed E. Abouelregal[1,3]

[1] Department of Mathematics, College of Science and Arts of Gurayyat, Jouf University, Gurayyat, Saudi Arabia

[2] Department of Mathematics, Faculty of Science of Monastir, Monastir University, Monastir, 5019, Tunisia, Email: saidi.anouar@yahoo.fr

[3] Department of Mathematics, Faculty of Science, Mansoura University, Mansoura, 35516, Egypt, Email: ahabogal@gmail.com

Received December 03 2019; Revised January 29 2020; Accepted for publication February 20 2020.
Corresponding author: A. Saidi (saidi.anouar@yahoo.fr)

Abstract. In this work, a generalized higher-order time-derivatives model with phase-lags has been introduced. This model is applied to study the thermal heat problem of a homogeneous and isotropic long cylinder due to initial stress and heat source. We use the Laplace transform method to solve the problem. The numerical solutions for the field functions are obtained numerically using the numerical Laplace inversion technique. The effect of the higher-order parameters, the initial stress, the magnitude of the heat source and the instant time on the temperature field, the displacement field, and the stress fields have been calculated and displayed graphically and the obtained results are discussed. The results are compared with those obtained previously in the contexts of some other models of thermoelasticity.

Keywords: Generalized thermoelasticity, Phase-lags, Higher-order, Initial stress.

1. Introduction

The theory of thermoelasticity deals with the effect of mechanical and thermal disturbances on an elastic body. It is concerned with the interaction among deformation and thermal fields. In the nineteenth century, Duhamel [1] and Neumann [2] announced the theory of uncoupled thermoelasticity. An important shortcoming of this theory is that the mechanical state of the elastic body does not affect the temperature which is not following true physical experiments. To surmount this paradox, Biot [3] in 1956 formulated the theory of coupled thermoelasticity by including inertia terms in the equation of motion. Also, to eliminate the contradiction in the coupled thermoelasticity theory (infinite speed of heat propagation), Cattaneo [4], Vernotte [5], Lord and Shulman [6], Green and Lindsay [7], Green and Naghdi [8-10] and others formulated generalized theories of thermoelasticity. Tzou [11-13] in 1995 formulated the theory of dual phase-lag (DPL), which describes the thermal interactions between the phonons and the electrons on the microscopic level as delaying sources causing the response delay on the macroscopic scale. The importance of the DPL model is that it can be applied to experimental results. Recently, many authors solved numerous problems in the context of the dual-phase-lag model [14-24].

As applications of thermoelasticity, Banerjee et al. [25] proved experimentally that thermoelastic instabilities occur in the presence of a liquid lubricant between two sliding solid surfaces. Also, Wong et al [26] demonstrated that the residual stress within a material can be detected and measured using the thermoelastic effect. Marin et al [27] studied the theory of micropolar thermoelastic bodies whose micro-particles possess microtemperatures. Marin and Craciun [28] proved, under weak restrictions, the unicity of solution for a boundary value problem in dipolar thermoelasticity to model composite materials.

Published online: March 08 2020

Studying the dynamic interaction of thermoelastic materials with additional parameters is very useful in investigating several concrete applications. For example, the effect of initial stresses regarding the thermal and mechanical state of a thermoelastic solid has been discussed as given in [29-37] for various reasons involving the variation of gravity, the temperature difference, the quenching process, etc. Likewise, the influence of a heat source in an elastic body was extensively studied [38-43] owing to its numerous engineering applications, such as materials processing, cutting and pulsed laser welding, case hardening, etc.

The objective of the current article is to introduce and investigate a new thermoelasticity model with higher-order time-derivatives and two-phase delays. This modified model can be denoted as the HDPL model. Recently, Abouelregal [44-46] constructed three new general thermoelastic heat conduction models including higher-order time-derivatives and two phase-lags. Zampol [47] proved the continuous dependence of the solution of suitable initial-boundary value problems with respect to initial given data for three different HDPL models. The same author studied the uniqueness of the solution in [48]. Chiriţă et al [49] studied the thermodynamical consistency of higher-order dual-phase-lag models of heat conduction.

To verify the accuracy of the current model, we have discussed a thermal heat problem for an infinitely long cylinder subjected to a decaying and periodic heat source and exposed to a constant hydrostatic initial stress. Expressions of the studied variables are calculated under appropriate initial conditions. Using the Laplace transform and numerical Laplace inversion, the problem is solved. The variations of temperature, displacement and thermal stress distributions are investigated through the influence of the higher-order time-derivative parameters, heat source magnitude, initial stress and instant time. The obtained numerical results are illustrated graphically and show that the analytic solutions are in good accordance with the numerical solutions. We believe that the analysis of this study will be useful to understand the basic features of this new model for heat conduction.

2. Governing Equations of Thermoelasticity Theory

The classical model of the Fourier's law ([6] and [50, 51]) states that the heat flux at any point in a body is proportional to the gradient of temperature at the same point, that is,

$$\mathbf{q}(x,t) = -K\nabla\theta(x,t) \tag{1}$$

where $\mathbf{q}$ is the heat flux, K is the thermal conductivity and $\theta = T - T_0$ represents the thermodynamic temperature in which T is the temperature-change above a uniform reference temperature T_0 of the body chosen such that $|T - T_0|/T_0 \ll 1$. Cattaneo [4], Vernotte [5], Lord and Shulman [6] formulated the theory of generalized thermoelasticity with one relaxation time by the equation

$$\mathbf{q}(x,t+\tau_{\mathrm{q}}) = -K\nabla\theta(x,t) \tag{2}$$

where τ_{q} is the single phase-lag. Also, Tzou [11-13] proposed a generalization of the Fourier's law with two phase-lags given by

$$\mathbf{q}(x,t+\tau_{\mathrm{q}}) = -K\nabla\theta(x,t+\tau_{\theta}) \tag{3}$$

where τ_{θ} is the phase-lag of the temperature gradient. The classical energy equation [52] is formulated by

$$-\nabla\cdot\mathbf{q} + \rho Q = \rho C_e\frac{\partial\theta}{\partial t} + \gamma T_0\frac{\partial e}{\partial t} \tag{4}$$

where C_e denotes the specific heat at constant strain, $\gamma = (3\lambda + 2\mu)\alpha_t$ represents the stress temperature modulus, in which α_t denotes the thermal expansion coefficient, λ and μ are Lamé's constants, ρ is the density of the medium and Q is the heat source per unit mass. In this work, a Taylor series approximation of Eq. (3) together with the energy equation (4) lead to a generalized heat equation describing a dual-phase-lag thermoelastic model. In the modified new model, Eq. (3) is approximated by

$$\left(1+\sum_{k=1}^{m}\frac{\tau_{\mathrm{q}}^{k}}{k!}\frac{\partial^{k}}{\partial t^{k}}\right)\mathbf{q}(x,t) = -K\left(1+\sum_{k=1}^{p}\frac{\tau_{\theta}^{k}}{k!}\frac{\partial^{k}}{\partial t^{k}}\right)\nabla\theta(x,t) \tag{5}$$

where p and m are finite number of terms of higher-order time-derivatives. Introducing Eq. (5) into Eq. (4), we obtain the modified equation of heat conduction with higher-order time-derivatives and two phase-lags as

$$K\left(1+\sum_{k=1}^{p}\frac{\tau_\theta^k}{k!}\frac{\partial^k}{\partial t^k}\right)\nabla.(\nabla\theta)=\left(1+\sum_{k=1}^{m}\frac{\tau_q^k}{k!}\frac{\partial^k}{\partial t^k}\right)\left(\rho C_e\frac{\partial\theta}{\partial t}+\gamma T_0\frac{\partial e}{\partial t}-\rho Q\right) \tag{6}$$

Equation (6) describes the coupled thermoelasticity theory, the Lord and Shulman theory and dual-phase-lag model for different values of the parameters τ_θ, τ_q and m, p as follows

(i) Coupled thermoelasticity (CTE) theory when $\tau_\theta = 0$ and $\tau_q = 0$.

(ii) Generalized theory with one relaxation time (LS) when $\tau_\theta = 0$ and $m = 1$.

(iii) Generalized theory with two phase-lags (DPL) when ($m = 2$, $p = 1$).

The other models, when $m > 2$ or $p > 1$, are called higher-order dual-phase-lag and denoted in this article by (HDPL). Quintanilla [53] proved that Eq. (5), in the case ($m = 2$, $p = 1$) with appropriate initial and boundary conditions for θ, conducts to an exponentially stable system if and only if $0 < \tau_q < 2\tau_\theta$. Fabrizio and Lazzari [54] has shown that the same model is compatible with the thermodynamics with the same restriction on τ_θ and τ_q. In this regard, Chirita et al. [49] proved that for the (HDPL) model ($m = 3$, $p = 2$) the restriction to be fulfilled in order to have the thermodynamic consistency is $0.28441\tau_\theta < \tau_q < 1.4902\tau_\theta$. Authors proved also that the model ($m = 4$, $p = 3$) is compatible with the thermodynamics provided that $0 < \tau_q < 1.33\tau_\theta$. Besides, the well posedness of dual and three-phase-lag models of heat conduction equation was considered by Wang et al [55-57] and Quintanilla [58-59].

Following [34-37], the additional governing equations for an isotropic homogenous thermoelastic solid with hydrostatic initial stress in the absence of external body forces are given below:

$$\sigma_{ij} = 2\mu e_{ij} + \lambda e_{kk}\delta_{ij} - \gamma\theta\delta_{ij} - P(\delta_{ij} + \omega_{ij}) \tag{7}$$

$$2e_{ij} = u_{j,i} + u_{i,j}, \quad 2\omega_{ij} = u_{j,i} - u_{i,j} \tag{8}$$

$$\sigma_{ij,j} = \rho\frac{\partial^2 u_i}{\partial t^2} \tag{9}$$

where σ_{ij} stands for the components of the stress tensor, e_{ij} stands for the components of the strain tensor, ω_{ij} is the rotation tensor, P is the initial stress and u_i is the component of the displacement vector.

3. Formulation of the Problem

We consider the problem of an infinitely long cylinder of radius a. The cylinder surface is due to hydrostatic initial stress, thermal shock and exposed to periodically and decaying heat source. We use the cylindrical coordinates (r, φ, z) with the z-axis lying along the axis of the cylinder (see Fig. 1).

Due to cylindrical symmetry, all the state functions can be expressed in terms of the radial distance r and the time t. Thus, the displacement vector has the components

$$u_r = u(r,t),\, u_\varphi(r,t) = u_z(r,t) = 0 \tag{10}$$

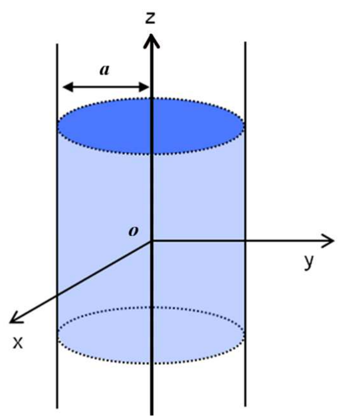

Fig. 1. Schematic diagram for the infinitely long cylinder.

The strain tensor has the following components

$$e_{rr} = \frac{\partial u}{\partial r}, \quad e_{\varphi\varphi} = \frac{u}{r}, \quad e_{r\varphi} = e_{rz} = e_{zz} = e_{\varphi z} = 0 \tag{11}$$

The cubic dilatation e is given by

$$e = \frac{1}{r}\frac{\partial(ru)}{\partial r} = \frac{\partial u}{\partial r} + \frac{u}{r} \tag{12}$$

By setting $i = j$ in Eq. (7), we obtain $\omega_{ij} = 0$ and $\delta_{ij} = 1$, then $P\left(\delta_{ij} + \omega_{ij}\right) = P$. Now, we replace the strain components in Eq. (7) by their values in (11). The non-vanishing constitutive relations of the system can be written as

$$\begin{aligned} \sigma_{rr} &= 2\mu\frac{\partial u}{\partial r} + \lambda e - \gamma\theta - P \\ \sigma_{\varphi\varphi} &= 2\mu\frac{u}{r} + \lambda e - \gamma\theta - P \\ \sigma_{zz} &= \lambda e - \gamma\theta - P \end{aligned} \tag{13}$$

In cylindrical coordinates, the equation of motion (9) can be expressed as (chapter 1 of [60])

$$\begin{aligned} &\frac{\partial \sigma_{rr}}{\partial r} + \frac{1}{r}\frac{\partial \sigma_{\varphi r}}{\partial \varphi} + \frac{\partial \sigma_{zr}}{\partial z} + \frac{\sigma_{rr} - \sigma_{\varphi\varphi}}{r} = \rho\frac{\partial^2 u_r}{\partial t^2} \\ &\frac{\partial \sigma_{r\varphi}}{\partial r} + \frac{\dfrac{\partial \sigma_{\varphi\varphi}}{\partial \varphi} + 2\sigma_{r\varphi}}{r} + \frac{\partial \sigma_{\varphi z}}{\partial z} = \rho\frac{\partial^2 u_\varphi}{\partial t^2} \\ &\frac{\partial \sigma_{rz}}{\partial r} + \frac{\dfrac{\partial \sigma_{\varphi z}}{\partial \varphi} + \sigma_{rz}}{r} + \frac{\partial \sigma_{zz}}{\partial z} = \rho\frac{\partial^2 u_z}{\partial t^2} \end{aligned} \tag{14}$$

Considering that $\sigma_{r\varphi} = \sigma_{rz} = \sigma_{\varphi z} = 0$, $u_\varphi = u_z = 0$ and that the stresses and strains depends only on r and t, Eq. (14) leads to

$$\frac{\partial \sigma_{rr}}{\partial r} + \frac{\sigma_{rr} - \sigma_{\varphi\varphi}}{r} = \rho\frac{\partial^2 u}{\partial t^2} \tag{15}$$

From Eqs. (12), (13) and (15), yields

$$(\lambda + 2\mu)\frac{\partial e}{\partial r} - \gamma\frac{\partial \theta}{\partial r} = \rho\frac{\partial^2 u}{\partial t^2} \tag{16}$$

Applying the operator $1/r\,\partial(r)/\partial r$ to both sides of Eq. (16), we get

$$(\lambda + 2\mu)\nabla^2 e - \gamma\nabla^2\theta = \rho\frac{\partial^2 e}{\partial t^2} \tag{17}$$

where the Laplacien operator ∇^2 is given by

$$\nabla^2 = \frac{1}{r}\frac{\partial}{\partial r} + \frac{\partial^2}{\partial r^2} \tag{18}$$

Also, the heat equation appeared in Eq. (6) turn out to be

$$K\left(1+\sum_{k=1}^{p}\frac{\tau_\theta^k}{k!}\frac{\partial^k}{\partial t^k}\right)\nabla^2\theta=\left(1+\sum_{k=1}^{m}\frac{\tau_q^k}{k!}\frac{\partial^k}{\partial t^k}\right)\left(\rho C_e\frac{\partial\theta}{\partial t}+\gamma T_0\frac{\partial e}{\partial t}-\rho Q\right) \tag{19}$$

We will use the following non-dimensional parameters

$$\begin{gathered}\{r',u'\}=c_1\eta\{r,u\},\quad \{t',\tau_q',\tau_\theta'\}=c_1^2\eta\{t,\tau_q,\tau_\theta\},\quad \theta'=\frac{\gamma}{\rho c_1^2}\theta\\ Q'=\frac{\gamma}{Kc_1^4\eta^2}Q,\quad \{\sigma_{ij}',P'\}=\frac{1}{\rho c_1^2}\{\sigma_{ij},P\},\quad \eta=\frac{\rho C_e}{K}\end{gathered} \tag{20}$$

where $c_1=\sqrt{(\lambda+2\mu)/\rho}$ is the dilatational wave velocity. Using the non-dimensional parameters (20), the equations (13), (17) and (19) reduce to (dropping the primes for convenience)

$$K\left(1+\sum_{k=1}^{p}\frac{\tau_\theta^k}{k!}\frac{\partial^k}{\partial t^k}\right)\nabla^2\theta=\left(1+\sum_{k=1}^{m}\frac{\tau_q^k}{k!}\frac{\partial^k}{\partial t^k}\right)\left(\frac{\partial\theta}{\partial t}+\varepsilon\frac{\partial e}{\partial t}-Q\right) \tag{21}$$

$$\nabla^2 e-\nabla^2\theta=\frac{\partial^2 e}{\partial t^2} \tag{22}$$

$$\begin{gathered}\sigma_{rr}=\beta^2\frac{\partial u}{\partial r}+\left(1-\beta^2\right)e-\theta-P\\ \sigma_{\varphi\varphi}=\beta^2\frac{u}{r}+\left(1-\beta^2\right)e-\theta-P\\ \sigma_{zz}=\left(1-\beta^2\right)e-\theta-P\end{gathered} \tag{23}$$

where

$$\beta^2=\frac{2\mu}{\lambda+2\mu},\quad \varepsilon=\frac{\gamma^2 T_0}{\rho^2 C_e c_1^2} \tag{24}$$

4. Initial and Boundary Conditions

The initial conditions of the problem are taken such that the medium is at rest and undisturbed initially as mentioned in the equation below

$$u(r,0)=\frac{\partial u(r,0)}{\partial t}=0,\quad \theta(r,0)=\frac{\partial\theta(r,0)}{\partial t}=0 \tag{25}$$

We suppose that the following boundary conditions are also hold:

(i) The surface of the cylinder is subjected to thermal shock of the form

$$\theta(a,t)=\theta_0 H(t),\ \ t>0 \tag{26}$$

where H is the Heaviside unit step function and θ_0 is a constant.

(ii) The surface of the cylinder is traction free

$$\sigma_{rr}(a,t)=0 \tag{٢7}$$

The cylinder is initially at zero temperature and for times $t>0$, the heat is generated or consumed within the cylinder at a time-dependent periodic and decaying generation rate as in [43], described by the equation

$$Q(r,t)=Q_0 t e^{-\frac{t}{2}}\cos(t), \tag{28}$$

in which Q_0 is the magnitude of the heat generation rate.

5. Solution of the Problem in the Laplace Transform Domain

The application of the Laplace transform technique changes the current problem from the unsteady to a steady one in the transform domain. Thus, Eqs. (21-23) can be written in the transform field as

$$\left(\nabla^2 - q\right)\overline{\theta} = q\varepsilon\overline{e} - q\frac{\overline{Q}}{s} \tag{29}$$

$$\left(\nabla^2 - s^2\right)\overline{e} = \nabla^2\overline{\theta} \tag{30}$$

$$\begin{aligned}
\overline{\sigma}_{rr} &= \beta^2\frac{\partial\overline{u}}{\partial r} + \left(1-\beta^2\right)\overline{e} - \overline{\theta} - \frac{\overline{P}}{s} \\
\overline{\sigma}_{\varphi\varphi} &= \beta^2\frac{\overline{u}}{r} + \left(1-\beta^2\right)\overline{e} - \overline{\theta} - \frac{\overline{P}}{s} \\
\overline{\sigma}_{zz} &= \left(1-\beta^2\right)\overline{e} - \overline{\theta} - \frac{\overline{P}}{s}
\end{aligned} \tag{31}$$

where

$$q = \frac{s\left(1+\sum_{k=1}^{m}\frac{\tau_q^k}{k!}s^k\right)}{\left(1+\sum_{k=1}^{p}\frac{\tau_\theta^k}{k!}s^k\right)}, \quad \overline{Q}(r,s) = \frac{4\left(-3+4s+4s^2\right)}{\left(5+4s+4s^2\right)^2} \tag{32}$$

Eliminating $\overline{\theta}$ from Eqs. (29) and (30), one gets

$$\left(\nabla^4 - A\nabla^2 + B\right)\overline{\theta} = C\overline{Q} \tag{33}$$

where the coefficients A, B and C are given by

$$A = s^2 + q + q\varepsilon, \quad B = qs^2, \quad C = qs \tag{34}$$

Since A and B are real positive numbers then Eq. (33) becomes

$$\left(\nabla^2 - m_1^2\right)\left(\nabla^2 - m_2^2\right)\overline{\theta} = C\overline{Q} \tag{35}$$

where m_1^2 and m_2^2 are the roots of the characteristic equation

$$m^4 - Am^2 + B = 0 \tag{36}$$

The solution of Eq. (33) can be written in the form

$$\overline{\theta} = \sum_{i=1}^{2} A_i I_0\left(m_i r\right) + \frac{\overline{Q}}{s} \tag{37}$$

where I_0 is the modified Bessel functions of the first kind of order zero and the parameters A_i, $\left(i = 1,2\right)$ can be determined from the boundary conditions. Similarly, the solution of $\overline{e}$ can be obtained as

$$\overline{e} = \frac{1}{q\varepsilon}\sum_{i=1}^{2} A_i\left(m_i^2 - q\right)I_0\left(m_i r\right) \tag{38}$$

In the Laplace transform domain, from Eqs. (12) and (38), we get

$$\overline{u} = \frac{1}{q\varepsilon}\sum_{i=1}^{2}\frac{A_i}{m_i}\left(m_i^2 - q\right)I_1\left(m_i r\right) \tag{39}$$

In deriving Eq. (39), we have used the following well-known relation of the Bessel function

$$\int x\, I_0(x)\, dx = x\, I_1(x) \tag{40}$$

Differentiating Eq. (39) with respect to r, we arrive at

$$\frac{\partial \bar{u}}{\partial r} = \frac{1}{q\varepsilon}\sum_{i=1}^{2} A_i\left(m_i^2 - q\right)\left(I_0\left(m_i r\right) - \frac{1}{r m_i} I_1\left(m_i r\right)\right) \tag{41}$$

In addition, the thermal stresses that appeared in Eq. (31) can be expressed as

$$\bar{\sigma}_{rr} = \sum_{i=1}^{2} A_i\left(\left(\frac{\left(m_i^2 - q\right)}{q\varepsilon} - 1\right) I_0\left(m_i r\right) - \left(\frac{\beta^2\left(m_i^2 - q\right)}{q\varepsilon r m_i}\right) I_1\left(m_i r\right)\right) - \frac{\bar{Q}}{s} - \frac{\bar{P}}{s} \tag{42}$$

$$\bar{\sigma}_{\varphi\varphi} = \sum_{i=1}^{2} A_i\left(\left(\frac{\left(1-\beta^2\right)\left(m_i^2 - q\right)}{q\varepsilon} - 1\right) I_0\left(m_i r\right) - \left(\frac{\beta^2\left(m_i^2 - q\right)}{q\varepsilon r m_i}\right) I_1\left(m_i r\right)\right) - \frac{\bar{Q}}{s} - \frac{\bar{P}}{s} \tag{43}$$

$$\bar{\sigma}_{zz} = \sum_{i=1}^{2} A_i\left(\frac{\left(1-\beta^2\right)\left(m_i^2 - q\right)}{q\varepsilon} - 1\right) I_0\left(m_i r\right) - \frac{\bar{Q}}{s} - \frac{\bar{P}}{s} \tag{44}$$

After applying Laplace transform, the boundary conditions (26) and (27) take the forms

$$\bar{\theta}(a,s) = \frac{\theta_0}{s}, \quad \bar{\sigma}_{rr}(a,s) = 0 \tag{45}$$

Substituting Eqs. (37) and (42) into the above boundary conditions, we get two equations in the unknown parameters $A_i, (i = 1, 2)$ as follows

$$\begin{gathered}\sum_{i=1}^{2} A_i I_0\left(m_i a\right) + \frac{\bar{Q}}{s} = \frac{\theta_0}{s} \\ \sum_{i=1}^{2} A_i\left(\left(\frac{\left(m_i^2 - q\right)}{q\varepsilon} - 1\right) I_0\left(m_i r\right) - \left(\frac{\beta^2\left(m_i^2 - q\right)}{q\varepsilon r m_i}\right) I_1\left(m_i r\right)\right) - \frac{\bar{Q}}{s} - \frac{\bar{P}}{s} = 0\end{gathered} \tag{46}$$

Solving this system, we obtain the values of the constants $A_i, (i = 1, 2)$. Hence, we obtain the expressions for the temperature, the displacement and the stress components of the medium in the Laplace transform domain.

6. Laplace Transform Inversion

In order to obtain the solutions of the different physical fields in the physical domain, it is necessary to perform Laplace inversion for the considered solutions obtained in the transformed domain. In this paper, an accurate and efficient numerical method proposed by Dubner and Abate [61] and based on a Fourier series expansion is used to obtain the inverse of the Laplace transform. An essential feature of this method is to be conceptually simple and easy to program. Specifically, authors have shown that any function f in Laplace domain takes the form $f(t) = f_c(t) - E(t)$ where f_c is the proposed approximation to f defined for $t \in [0, T]$ by

$$f_c(t) = 2\frac{e^{ct}}{T}\left(\frac{1}{2}\bar{f}(r,c) + \mathrm{Re}\sum_{p=1}^{\infty}\bar{f}\left(r, c + \frac{ip\pi}{T}\right)\cos\left(\frac{p\pi}{T}t\right)\right) \tag{47}$$

Re is the real part, i is imaginary number unit and c is any real positive number. In the same article [61], authors have shown that the error term E can be made conveniently small by appropriately choosing the parameter c and only for $t \le T/2\cdot$ If one takes $t = T/2$ in (47), then f can be approximated to

$$f_c(t) = \frac{e^{ct}}{t}\left(\frac{1}{2}\bar{f}(r,c) + \mathrm{Re}\sum_{n=1}^{N}\bar{f}\left(r, c + \frac{in\pi}{t}\right)(-1)^n\right) \tag{48}$$

where N is a finite number of terms.

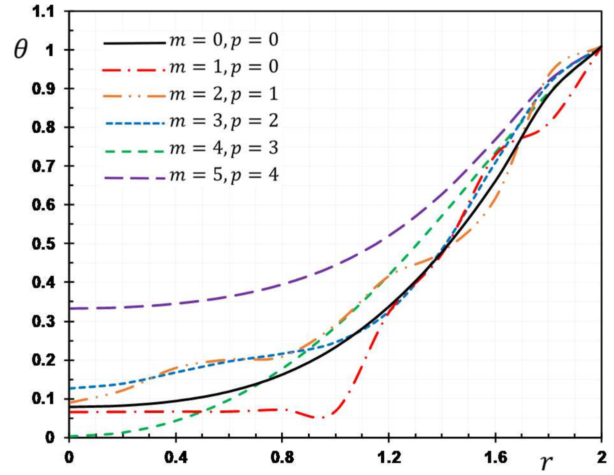

Fig. 2. Variation of the temperature θ versus the radius r for different models of thermoelasticity

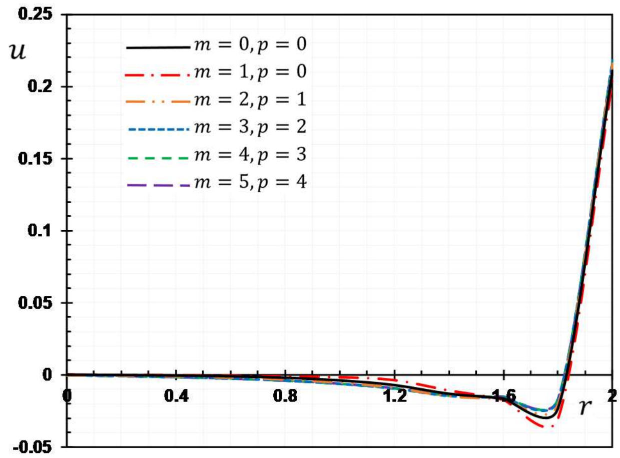

Fig. 3. Variation of the displacement u versus the radius r for different models of thermoelasticity

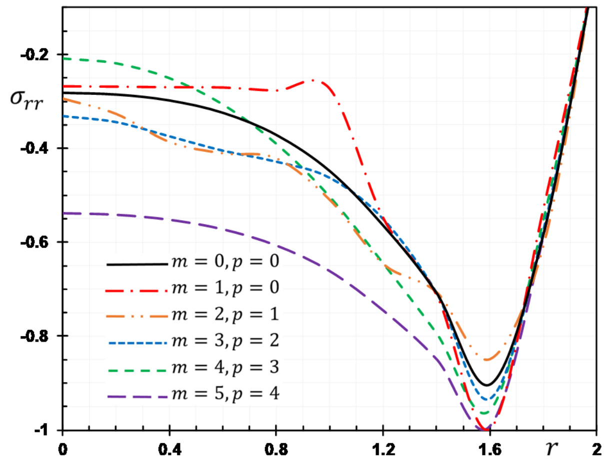

Fig. 4. Variation of the radial stress σ_{rr} versus the radius r for different models of thermoelasticity

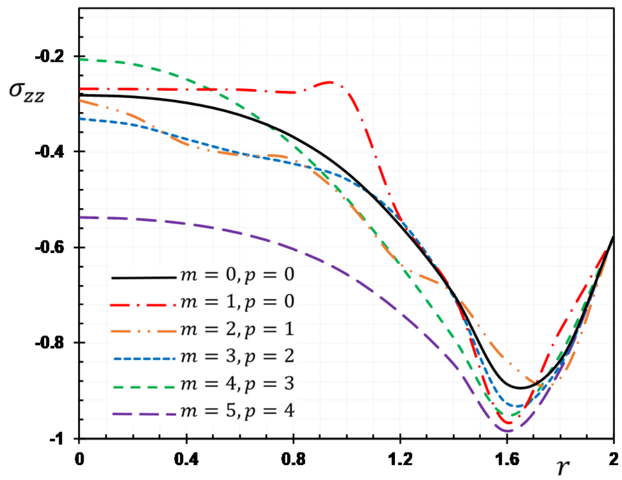

Fig. 5. Variation of the axial stress σ_{zz} versus the radius r for different models of thermoelasticity

7. Numerical Results

To illustrate the theoretical results obtained in the preceding section, we now present some computational numerical results. For this objective, the copper material was chosen as the thermal material. The physical constants of the copper material are given as [62-65]:

$$\begin{gathered}\lambda = 7.76\times 10^{10}\left(\mathrm{kg\,m^{-1}\,s^{-2}}\right),\quad \mu = 3.86\times 10^{10}\left(\mathrm{kg\,m^{-1}\,s^{-2}}\right),\quad \rho = 8954\left(\mathrm{kg\,m^{-3}}\right),\\ K = 386\left(\mathrm{W\,m^{-1}\,K^{-1}}\right),\quad C_e = 383.1\left(\mathrm{J\,kg^{-1}\,K^{-1}}\right),\quad T_0 = 293\left(\mathrm{K}\right),\quad \alpha_t = 1.78\times 10^{-5}\left(\mathrm{K^{-1}}\right).\end{gathered} \tag{49}$$

The computation was performed when $t = 0.2$, $\theta_0 = 1$, $\tau_q = 0.05$, $\tau_\theta = 0.1$ (which satisfies the thermodynamic consistency conditions given in [49]). The numerical technique outlined above was used to obtain temperature θ, radial displacement u, radial and axial stresses σ_{rr} and σ_{zz} inside the cylinder $(a = 2)$. These distributions are illustrated in Figs. 2-17. The current results are well consistent with the analytical solution. Numerical calculations are performed for four cases as follows:

7.1 The effect of higher-order parameters m and p.

In this case, we will study the effect of the higher-order parameters m and p on the different physical fields in the direction of the radius r along the interval $0 \le r \le 2$ when the other parameters remain constant: $Q_0 = 2.5$ (magnitude of the heat generation rate), $P = 0.2$ (initial stress). We will also compare the results obtained in the new model HDPL $(m > 2, p > 1)$

with the previous models CTE $(m=0, p=0)$, LS $(m=1, p=0)$ and DPL $(m=2, p=1)$. The numerical results and graphics are represented in Fig.2-5. From the figures, we note that m and p have a significant effect on the physical fields studied except for the displacement where the effect is weak. Also, the values in the modified model of thermoelasticity (HDPL model) are different compared with other models (CTE, LS and DPL).

The effect of higher-order parameters m and p plays an important role in all studied fields and the results in this work can be used to design various devices depending on the choice of m and p. It also appears from the figures that we must stop at $(m=4, p=3)$ to obtain acceptable physical results, which is in line with what has been proved by Chirita et al. [49] who have verified that for $m \geq 5$ or $p \geq 5$ the equivalent models unavoidably lead to unbalanced mechanical systems.

It is evident from Fig. 2 that the parameters m and p have a great effect on the thermodynamic temperature θ. Inside the cylinder, the solutions are different but the curves have a similar behavior except for the case $(m=5, p=4)$ which clearly presents higher values than the other models. More precisely, the temperature θ starts at maximum value $\theta \approx 1$ on the surface of the cylinder $r = 2$, (which satisfies the thermal boundary condition of the problem and ensures that the numerical method used here is very reliable). Then, the value gradually decreases by decreasing the radius r.

It is clear from Fig. 3 that the parameters m and p has a weak influence on the radial displacement u. Moreover, we observe that the variation of u corresponding to different values of m and p follows an almost similar pattern with a small difference in magnitudes limited to a bounded region $(0.8 \leq r \leq 1.8)$. Outside this region, the variation will disappear identically. Figure 3 shows that the displacement profile for different models starts at a common maximum value on the boundary of the cylinder, after that, it decreases rapidly to attain a small negative minimum value (near $r = 1.8$) and finally, increases gradually until it reaches zero value.

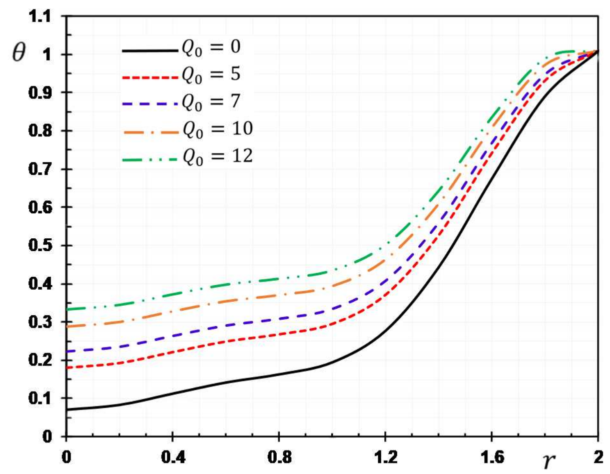

Fig. 6. Variation of the temperature θ versus radius r for different values of the magnitude Q_0 of the heat source

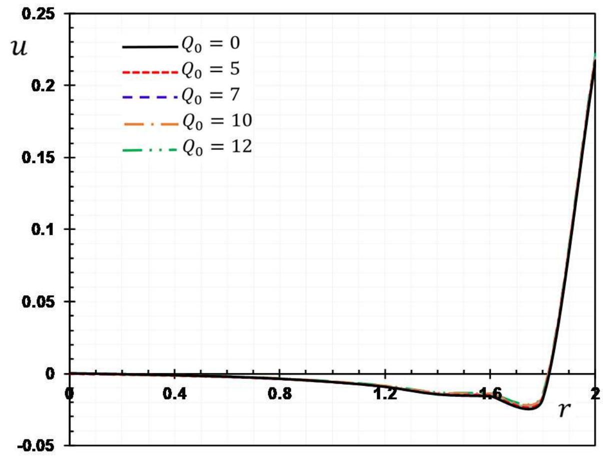

Fig. 7. Variation of the displacement u versus radius r for different values of the magnitude Q_0 of the heat source

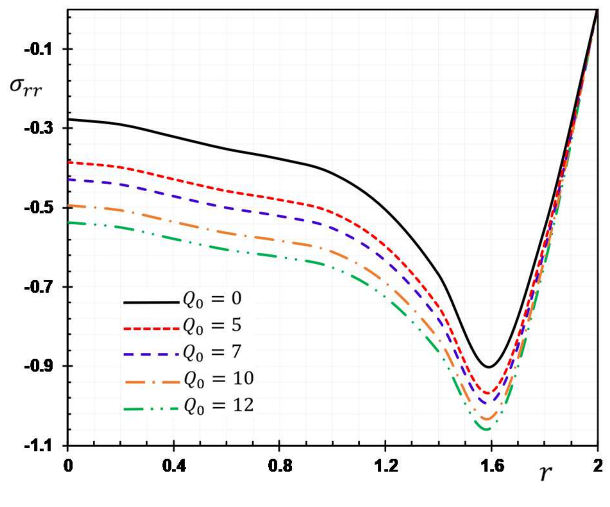

Fig. 8. Variation of the radial stress σ_{rr} versus radius r for different values of the magnitude Q_0 of the heat source

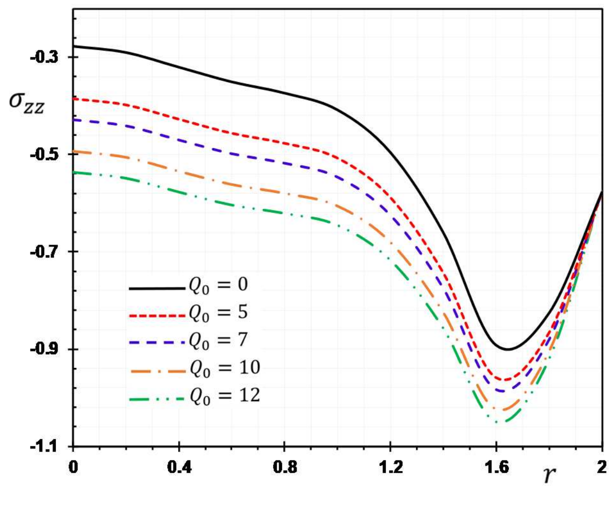

Fig. 9. Variation of the axial stress σ_{zz} versus radius r for different values of the magnitude Q_0 of the heat source

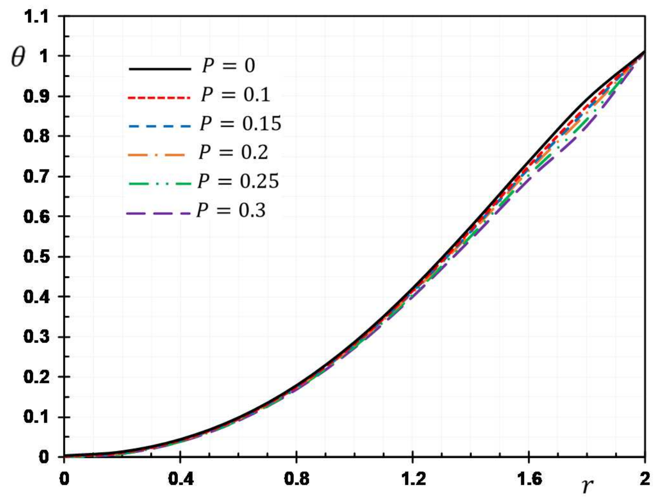

Fig. 10. Variation of the temperature θ versus radius r for different values of the the initial stress P

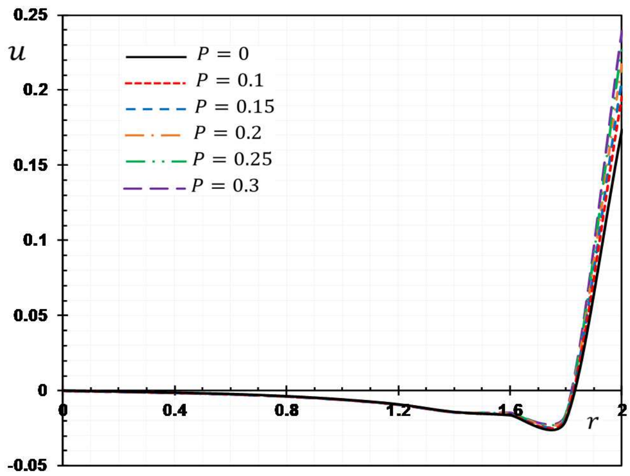

Fig. 11. Variation of the displacement u versus radius r for different values of the the initial stress P

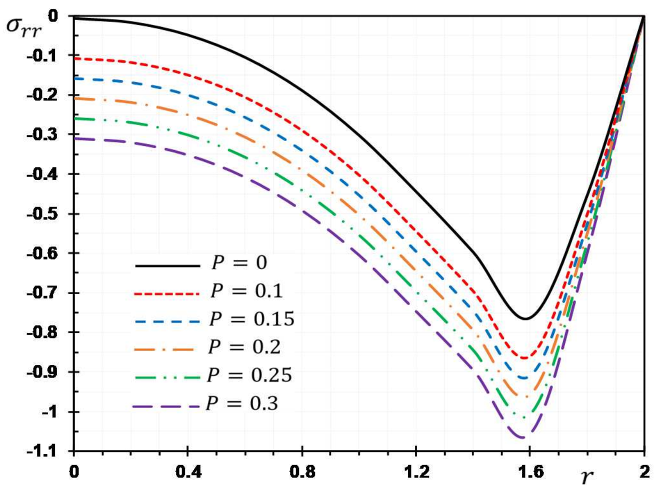

Fig. 12. Variation of the radial stress σ_{rr} versus radius r for different values of the the initial stress P

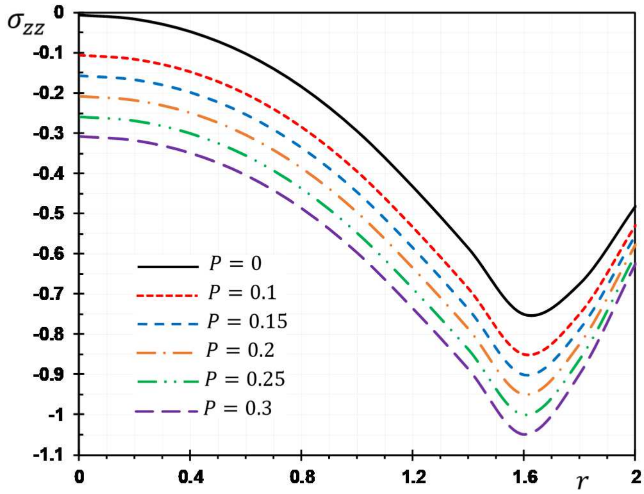

Fig. 13. Variation of the axial stress σ_{zz} versus radius r for different values of the the initial stress P

Figures 4 and 5 show the variations of thermal stresses σ_{rr} and σ_{zz} with respect to the distance r for different models of thermoelasticity. We notice that the parameters m and p have a significant effect on the profiles of σ_{rr} and σ_{zz}. In addition, it is clear that the solutions are different but the curves have a similar behavior except for the case $(m=5, p=4)$ which clearly presents, inside the cylinder, lower values than the other models.

It is obvious from Fig. 4 that the graph of σ_{rr} starts with a zero value which is consistent with the mechanical boundary conditions. Also, we note that it decreases rapidly with decreasing r in the range $1.6 \le r \le 2$ and then increases gradually with decreasing r until it reaches steady-state. The initial stress of the system explains the fact that this steady-state is different from zero. We note from Fig. 5 that the profile of σ_{zz} starts with a common negative value $\sigma_{zz} \approx -0.57$ and then follows an identical behavior to the profile of σ_{rr}.

7.2 The effect of the magnitude of the heat generation rate

This case illustrates how different physical fields vary in the direction of the radius r inside the cylinder with different values of the magnitude parameter of the heat source Q_0 in the context of the HDPL model $(m=3, p=2)$ when $P=0.2$. For this case, results and graphics are represented in Figs. 6-9. From these figures, we note that the parameter Q_0 has a significant effect on the studied physical fields except for displacement where the effect is weak. It is evident from Fig. 6 that θ increases with the increase of the parameter Q_0 and that the curves have a similar behavior. Figure 7 shows that the variation of the displacement u increases slightly with the increase of the parameter Q_0. From Figs. 8 and 9 it is observed that the stresses σ_{rr} and σ_{zz} decrease with increasing of the parameter Q_0. All these results match with the numerical results of [42].

7.3 The effect of the initial stress

This case explains how different studied fields differ with different values of the initial stress *P* in the context of the HDPL model. In this case, we take $m = 4, p = 3$ and $Q_0 = 2.5$. Numerical results and graphics are illustrated in Figs. 10-13. From these figures, we note that the parameter *P* has a significant effect on the thermal stresses σ_{rr} and σ_{zz} and weak influence on the temperature θ and the displacement *u*. It is evident from Fig. 10 that θ decreases slightly with the increase of the parameter *P* and that the curves have a similar behavior. Figure 11 shows that the variation of the displacement *u* increases slightly with the increase of the parameter *P*. From Figs. 12 and 13 it is observed that the stresses σ_{rr} and σ_{zz} decrease with increasing of the parameter *P* and that the curves have similar behavior. These results agree with the numerical result of [32].

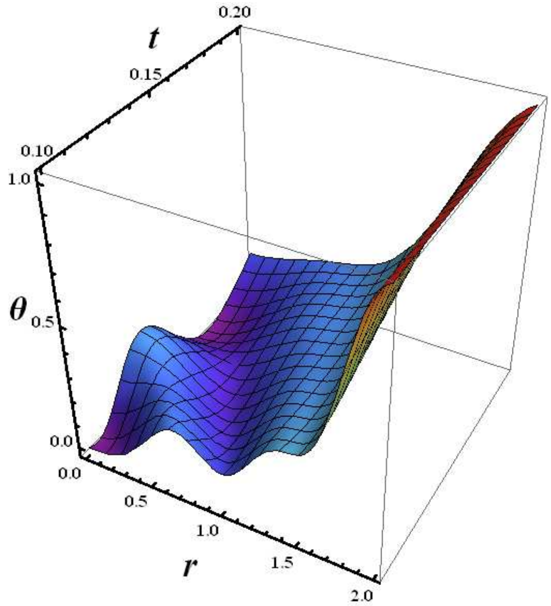

Fig. 14. Variation of the temperature θ versus radius *r* and instant time *t*

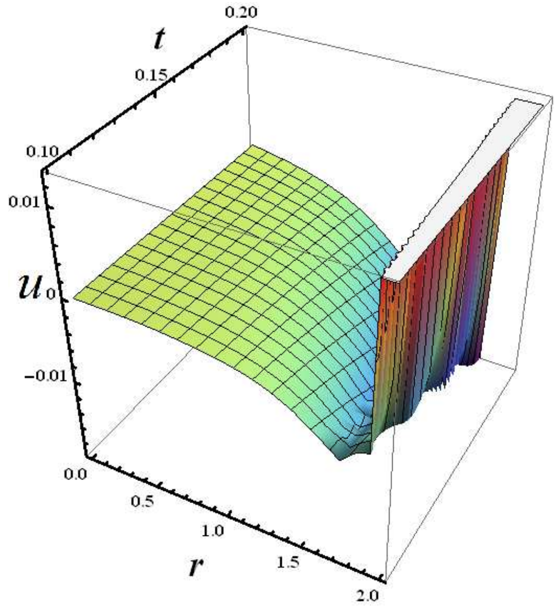

Fig. 15. Variation of the displacement *u* versus radius *r* and instant time *t*

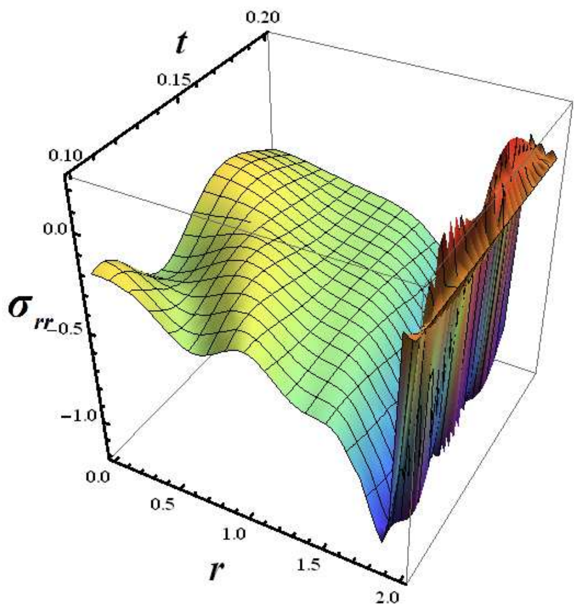

Fig. 16. Variation of the radial stress σ_{rr} versus radius *r* and instant time *t*

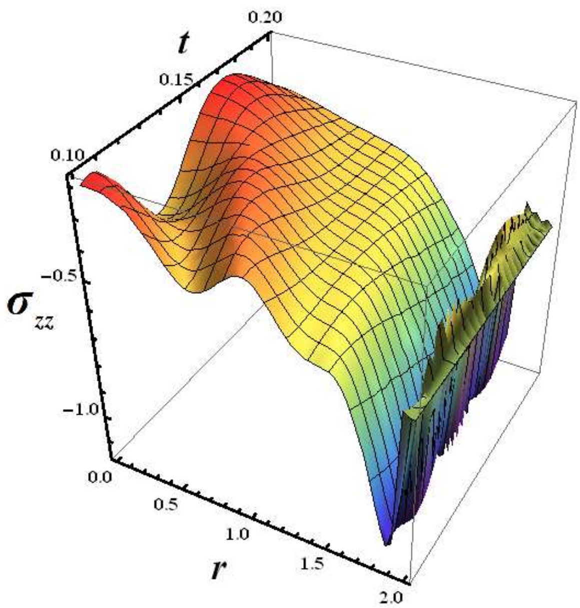

Fig. 17. Variation of the the axial stress σ_{zz} versus radius *r* and instant time *t*

7.4 The effect of the instant time

The last case illustrates how the non-dimensional temperature, displacement, and thermal stresses differ with different values of the instant time t in the range $0.1 \leq t \leq 0.2$ in the situation of the HDPL model $(m = 3, p = 2)$, and when the initial stress P and the magnitude Q_0 remain constant (P = 0.2 and Q_0 = 2.5). The values of different fields are plotted in Figs. 14-17. The influence of the instant time parameter t is much manifest in all physical fields distributions. It is detected that all studied fields attains their boundary values conditions recommended in the model.

Figure 14 shows that the temperature θ increases inside the cylinder with the increase of the parameter t to attain a maximum value at the instant $t \approx 0.13$, then it decreases until the instant $t \approx 0.17$ and finally increases slightly. However, the parameter t presents a weak influence on the temperature θ on the surface of the cylinder and the value of θ is equal to 1 which agrees with the boundary condition (26). We observe, from Fig. 15, that the parameter t presents a weak influence on the displacement u inside the cylinder. Also, the value of u is almost equal to 0 at r = 0. Moreover, the displacement u decreases slightly with the increase of t on the surface of the cylinder. It is evident from Fig. 16 and 17 that the stresses σ_{rr} and σ_{zz} decrease inside the cylinder with the increase of the parameter t to attain a minimum value at the instant $t \approx 0.13$, then they increase until the instant $t \approx 0.17$ and finally decreases again. However, the parameter t presents a weak effect on the thermal stresses on the surface of the cylinder. Indeed, the value of σ_{rr} is equal to 0 which is consistent with the mechanical boundary condition (27).

8. Conclusion

In this work, a thermoelastic model with higher-order time-derivatives and two phase-lags for an infinitely long cylinder under initial stress has been investigated. The medium is subjected to thermal shock as well as a periodic and decaying generation rate. All the associated equations have been completely solved using the Laplace transform technique and an accurate numerical inversion method. A comparison is made to show the dependence of all field variables on the higher-order parameter m and p associated with the different models of thermoelasticity (CTE, LS, DPL and HDPL). The effects of the time-dependent heat source and the hydrostatic initial stress are also discussed. From the numerical results, most fields are very sensitive to the variation of the parameters m and p, the heat source and the applied initial stress. The results are physically acceptable and accurate for the different models of thermoelasticity and especially when (m = 4, p = 3). The validity of results is acceptable by comparing the temperature, displacement, and thermal stresses according to the higher-order dual-phase-lag model with those due to other thermoelasticity models. The results presented in this article are useful to a wide range of problems in material science such as the design of new materials, bioheat transfer mechanisms between tissues and blood during non-equilibrium processes and drug delivery in tumors involving the heat and mass transfer in biological systems.

Author Contributions

All authors discussed the results, reviewed and approved the final version of the manuscript.

Conflict of Interest

The authors declared no potential conflicts of interest with respect to the research, authorship and publication of this article.

Funding

The authors received no financial support for the research, authorship and publication of this article.

Nomenclature

λ, μ	Lamé's constants [$\mathrm{kg\,m^{-1}\,s^{-2}}$]	K	Thermal conductivity [$\mathrm{W\,m^{-1}\,K^{-1}}$]
α_t	Thermal expansion coefficient [$\mathrm{K^{-1}}$]	ρ	Density of the medium [$\mathrm{kg\,m^{-3}}$]
C_e	Specific heat at constant strain [$\mathrm{J\,kg^{-1}\,K^{-1}}$]	Q	Heat source [$\mathrm{m^2\,s^{-3}}$]
T_0	Environmental temperature [K]	P	Initial stress [$\mathrm{kg\,m^{-1}\,s^{-2}}$]
T	Absolute temperature [K]	t	The time instant [s]
θ	Thermodynamic temperature [K]	τ_q	Phase lag of heat flux [s]
u	Radial component of the displacement vector [m]	τ_θ	Phase lag of temperature [s]

e	Cubical dilatation	$\gamma = (3\lambda + 2\mu)\alpha_t$	stress temperature modulus [$\mathrm{kg\,m^{-1}s^{-2}K^{-1}}$]
σ_{ij}	Stress tensor [kg $\mathrm{m^{-1}s^{-2}}$]	(r,φ,z)	Cylindrical coordinate
e_{ij}	Strain tensor	c_1	Dilatational wave velocity [m $\mathrm{s^{-1}}$]
q	Heat flux vector [kg $\mathrm{s^{-3}}$]		

References

[1] Duhamel, J.H., Second mémoire sur les phénomènes thermo-mécaniques, *Journal de L'Ecole Polytechnique*, 15(25), 1837, 1-57.
[2] Neumann, F.E., *Vorlesungen über die theorie der elasticität der festen körper und des lichtäthers,* Leipzig, B. G. Teubner, 1885.
[3] Biot, M.A., Thermoelasticity and Irreversible thermodynamics, *Journal of Applied Physics*, 27(3), 1956, 240–253.
[4] Cattaneo, C., Sur une forme de l'équation de la chaleur éliminant le paradoxe d'une propagation instantanée, *Comptes Rendus de l'Académie des Sciences*, 247, 1958, 431–433.
[5] Vernotte, P., Les paradoxes de la théorie continue de l'équation de la chaleur, *Comptes Rendus de l'Académie des Sciences*, 246, 1958, 3154–3155.
[6] Lord, H.W., Shulman, Y., A generalized dynamic theory of thermoelasticity, *Journal of the Mechanics and Physics of Solids*, 15(5), 1967, 299–309.
[7] Green, A.E., Lindsay, K.A., Thermoelasticity, *Journal of Elasticity*, 2(1), 1972, 1–7.
[8] Green, A.E., Naghdi, P.M., A Re-Examination of the basic postulates of thermomechanics, *Proceedings: Mathematical and Physical Sciences*, 432(1885), 1991, 171–194.
[9] Green, A.E., Naghdi, P.M., On undamped heat waves in an elastic solid, *Journal of Thermal Stresses*, 15(2), 1992, 253–264.
[10] Green, A.E., Naghdi, P.M., Thermoelasticity without energy dissipation, *Journal of Elasticity*, 31(3), 1993, 189–208.
[11] Tzou, D.Y., A unified approach for heat conduction from macro-to micro-scales, *Journal of Heat Transfer,* 117(1), 1995, 8–16.
[12] Tzou, D.Y., The generalized lagging response in small-scale and high-rate heating, *International Journal of Heat and Mass Transfer*, 38(17), 1995, 3231–3240.
[13] Tzou, D.Y., Experimental support for the lagging behavior in heat propagation, *Journal of Thermophysics and Heat Transfer*, 9(4), 1995, 686–693.
[14] Abdallah, I.A., Dual phase-lag heat conduction and thermoelastic properties of a semi-infinite medium induced by ultrashort pulsed laser, *Progress in Physics*, 2009(3), 2009, 60–63.
[15] Zenkour, A.M., Mashat, D.S., Abouelregal, A.E., The effect of dual-phase-lag model on reflection of thermoelastic waves in a solid half space with variable material properties, *Acta Mechanica Solida Sinica*, 26(6), 2013, 659–670.
[16] El-Karamany, A.S., Ezzat, M.A., On the dual-phase-lag thermoelasticity theory, *Meccanica*, 49(1), 2014, 79–89.
[17] Ezzat, M.A., El-Karamany, A.S., Ezzat, S.M., Two temperature theory in magneto-thermoelasticity with fractional order dual-phase-lag heat transfer, *Nuclear Engineering and Design*, 252, 2012, 267–277.
[18] Abbas, I.A., Zenkour, A.M., Dual-phase-lag model on thermoelastic interactions in a semi-infinite medium subjected to a ramp-type heating, *Journal of Computational and Theoretical Nanoscience,* 11(3), 2014, 642–645.
[19] Abd-Alla, A.M., Othman, M.I.A., and Abo-Dahab S.M., Reflection of plane waves from electro-magneto-thermoelastic half-space with a dual-phase-lag model, *Computers, Materials and Continua*, 51(2), 2016, 63–79.
[20] Aboulregal, A.E., Zenkour, A.M., Two-temperature thermoelastic surface waves in micropolar thermoelastic media via dual phase-lag model, *Advances in Aircraft and Spacecraft Science*, 4(6), 2017, 711–727.
[21] Zenkour, A.M., A generalized thermoelastic dual-phase-lagging response of thick beams subjected to harmonically varying heat and pressure, *Journal of Theoretical and Applied Mechanics*, 56(1), 2018, 15–30.
[22] Abouelregal A.E., Abo-Dahab S.M., A two-dimensional problem of a mode-I crack in a rotating fibre-reinforced isotropic thermoelastic medium under dual-phase-lag model, *Sādhanā*, 43(1), 2018, 1–11.
[23] Abouelregal, A.E., Abo-Dahab.S.M., Dual phase lag model on magneto-thermoelasticity infinite non-homogeneous solid having a spherical cavity, *Journal of Thermal Stresses*, 35(9), 2012, 820–841.
[24] Abouelregal, A.E., Abo-Dahab, S.M., Dual-phase-lag diffusion model for Thomson's phenomenon on elctromagneto-thermoelastic an infinitely long solid cylinder, *Journal of Computational and Theoretical Nanoscience,* 11(4), 2014, 1031–1039.
[25] Banerjee, B.N., Burton, R.A., Thermoelastic instability in lubricated sliding between solid surfaces, *Nature*, 261(3), 1976, 399-400.
[26] Wong, A.K., Dunn, S.A., Sparrow, J.G., Residual stress measurement by means of the thermoelastic effect, *Nature*, 332(6165), 1988, 613-615.
[27] Marin, M., Baleanu, D., Vlase, S., Effect of microtemperatures for micropolar thermoelastic bodies, *Structural Engineering and Mechanics*, 61(3), 2017, 381-387.
[28] Marin, M., Craciun, E.M., Uniqueness results for a boundary value problem in dipolar thermoelasticity to model composite materials, *Composites Part B: Engineering*, 126, 2017, 27-37.

[29] Mahmoud, S.R., An analytical solution for effect of magnetic field and initial stress on an infinite generalized thermoelastic rotating nonhomogeneous diffusion medium, *Abstract and Applied Analysis*, 2013, Article ID 284646, 2013, 1–11.
[30] Abd-Alla, A.M., Abo-Dahab, S.M., Effect of rotation and initial stress on an infinite generalized magneto-thermoelastic diffusion body with a spherical cavity, *Journal of Thermal Stresses*, 35(10), 2012, 892–912.
[31] Atwa, S.Y., Generalized magneto-thermoelasticity with two temperature and initial stress under Green–Naghdi theory, *Applied Mathematical Modelling*, 38(21-22), 2014, 5217–5230.
[32] Hussien, N., Abo-Dahab, S. M., Bayones, F. S., Effect of initial Stress, rotation and magnetic stress on isotropic elastic hollow cylinder, *Journal of Computational and Theoretical Nanoscience,* 12(8), 2015, 1615–1623.
[33] Lotfy, K., Hassan, W., Gabr, M.E., Thermomagnetic effect with two temperature theory for photothermal process under hydrostatic initial stress, *Results in Physics*, 7, 2017, 3918–3927.
[34] Montanaro, A. On singular surfaces in isotropic linear thermoelasticity with initial stress, *The Journal of the Acoustical Society of America*, 106(3), 1999, 1586–1588.
[35] Singh, B., Kumar, A., Singh, J. Reflection of generalized thermoelastic waves from a solid half-space under hydrostatic initial stress, *Applied Mathematics and Computation*, 177(1), 2006, 170–177.
[36] Othman M.I.A., Song Y.Q., Reflection of plane waves from an elastic solid half-space under hydrostatic initial stress without energy dissipation, *International Journal of Solids and Structures,* 44(17), 2007, 5651–5664.
[37] Singh, B., Effect of hydrostatic initial stresses on waves in a thermoelastic solid half-space, *Applied Mathematics and Computation*, 198(2), 2008, 494–505.
[38] Youssef, H.M., Two-temperature generalized thermoelastic infinite medium with cylindrical cavity subjected to moving heat source, *Archive of Applied Mechanics*, 80(11), 2009, 1213–1224.
[39] He, T., Cao, L., A problem of generalized magneto-thermoelastic thin slim strip subjected to a moving heat source, *Mathematical and Computer Modelling*, 49(7-8), 2009, 1710–1720.
[40] Youssef, H.M., Al-Lehaibi, E.A.N., The boundary value problem of a three-dimensional generalized thermoelastic half-space subjected to moving rectangular heat source, *Boundary Value Problems*, 2019(8), 2019.
[41] Xiong, C., Guo, Y., Effect of variable properties and moving heat source on magnetothermoelastic problem under fractional order thermoelasticity, *Advances in Materials Science and Engineering*, 2016, Article ID 5341569, 1–12.
[42] Abbas I.A., The effects of relaxation times and a moving heat source on a two-temperature generalized thermoelastic thin slim strip, *Canadian Journal of Physics*, 93(5), 2015, 585–590.
[43] Apatay, T., Exact solution to elastic behavior of periodic heat generating solid cylinder, *Journal of Polytechnic*, 19(4), 2016, 421-426.
[44] Abouelregal, A.E., On Green and Naghdi thermoelasticity model without energy dissipation with higher order time differential and phase-lags, *Journal of Applied and Computational Mechanics*, 6(3), 2020.
[45] Abouelregal, A.E., Two-temperature thermoelastic model without energy dissipation including higher order time-derivatives and two phase-lags, *Materials Research Express*, 6(11), 2019, 116535.
[46] Abouelregal, A.E., Modified fractional thermoelasticity model with multi-relaxation times of higher order: application to spherical cavity exposed to a harmonic varying heat, *Waves in Random and Complex Media*, 2019, doi: 10.1080/17455030.2019.1628320.
[47] Zampoli, V., Some continuous dependence results about high order time differential thermoelastic models, *Journal of Thermal Stresses*, 41(7), 2018, 827-846.
[48] Zampoli, V., Uniqueness theorems about high-order time differential thermoelastic models, *Ricerche di Matematica*, 67(2), 2018, 929–950.
[49] Chiriţă, S., Ciarletta, M., Tibullo, V., On the thermomechanical consistency of the time differential dual-phase-lag models of heat conduction, *International Journal of Heat and Mass Transfer*, 114, 2017, 277–285.
[50] Chandrasekharaiah, D.S., Thermoelasticity with second sound: a review, *Applied Mechanics Review*, 39(3), 1986, 355-376.
[51] Ghazanfarian, J., Shomali, Z., Abbassi, A., Macro- to nanoscale heat and mass transfer: the lagging behavior, *International Journal of Thermophysics,* 36(7), 2015, 1416–1467.
[52] Roy Choudhuri, S.K., On a thermoelastic three-phase-lag model, *Journal of Thermal Stresses*, 30(3), 2007, 231-238.
[53] Quintanilla, R., Exponential stability in the dual-phase-lag heat conduction theory, *Journal of Non-Equilibrium Thermodynamics*, 27(3), 2002, 217–227.
[54] Fabrizio, M., Lazzari, B., Stability and second law of thermodynamics in dual-phase-lag heat conduction*, International Journal of Heat and Mass Transfer,* 74, 2014, 484–489.
[55] Wang, L., Xu, M., Zhou, X., Well-posedness and solution structure of dual-phase-lagging heat conduction, *International Journal of Heat and Mass Transfer*, 44, 2001, 1659–1669.
[56] Wang, L., Xu, M., Well-posedness of dual-phase-lagging heat conduction equation: higher dimensions, *International Journal of Heat and Mass Transfer*, 45, 2002, 1165–1171.
[57] Xu, M., Wang, L., Thermal oscillation and resonance in dual-phase-lagging heat conduction, *International Journal of Heat and Mass Transfer*, 45, 2002, 1055–1061.
[58] Quintanilla, R., A well posed problem for the dual-phase-lag heat conduction, *Journal of Thermal Stresses*, 31(3), 2008, 260–269.

[59] Quintanilla, R., A well-posed problem for the three-dual-phase-lag heat conduction, *Journal of Thermal Stresses*, 32(12), 2009, 1270–1278.
[60] Nowaski, W., *Thermoelasticity*, Pergamon Press, 1986.
[61] Dubner, H., Abate, J., Numerical inversion of Laplace transforms by relating them to the finite Fourier cosine transform, *Journal of the ACM,* 15(1), 1968, 115–123.
[62] Sokolnikoff, I.S., *Mathematical Theory of Elasticity*, New York, Dover, 1946.
[63] Thomas, L.C., *Fundamentals of Heat Transfer*, Prentice-Hall Inc., Englewood Cliffs, New Jersey, 1980.
[64] Abouelregal, A.E., Fractional heat conduction equation for an infinitely generalized thermoelastic long solid cylinder, *International Journal for Computational Methods in Engineering Science and Mechanics*, 17(5-6), 2016, 374–381.
[65] Aouadi, M., A problem for an infinite elastic body with a spherical cavity in the theory of generalized thermoelastic diffusion, *International Journal of Solids and Structures*, 44(17), 2007, 5711–5722.

ORCID iD

Anouar Saidi https://orcid.org/0000-0002-1147-5488
Ahmed E. Aboueregal https://orcid.org/0000-0003-3363-7924

How to cite this article: Saidi A., Aboueregal A.E. Thermoelastic Model with Higher-order Time-derivatives and Two Phase-lags for an Infinitely Long Cylinder under Initial Stress and Heat Source, *J. Appl. Comput. Mech.*, 7(1), 2021, 277–291. https://doi.org/10.22055/JACM.2020.31836.1924